Surface Melting of Ice I_h Single Crystals Revealed by Glancing Angle X-Ray Scattering

A. Lied,[1,2] H. Dosch,[1,*] and J. H. Bilgram[3]

[1]*Sektion Physik der Universität München, D-80539 München, West Germany*

[2]*Institut Laue-Langevin, F-38042 Grenoble Cedex, France*

[3]*Institut für Festkörperphysik der Eidgenössische Technische Hochschule Zürich-Hönggerberg, CH-8093 Zürich, Switzerland*

(Received 8 November 1993)

We present glancing angle x-ray scattering experiments at [00.1], [10.0], and [11.0] surfaces of ice I_h single crystals. The temperature dependence of the evanescent Bragg scattering upon heating reveals a quasiliquid surface layer well below the melting point on each investigated ice surface. At [10.0] and [11.0] surfaces, thermal faceting is observed, which is briefly discussed. The "oxygen-forbidden" (00.4) Bragg profiles which give direct access to hydrogen long-range order have been investigated in the bulk and close to the surface. Although in the bulk the (00.4) width is resolution limited, we discovered prior to surface melting a strong rotational disorder of the hydrogen bonds within a mesoscopic surface sheet.

PACS numbers: 64.70.Dv, 61.10.Lx, 68.45.Gd

The possibility that a mesoscopic liquid layer exists at ice surfaces well below the melting point has been fascinating scientists since it was suggested by Faraday in 1859 [1]. It has been argued that this so-called surface melting of ice plays a fundamental role in many phenomena of our everyday life as in the charge transfer in thunderstorms [2], in frost heave [3], or in skiing and skating [4]. Accordingly many attempts have been undertaken to directly observe this surface disordering process [5–9]. Early friction and adhesion measurements provided indirect evidence for a liquidlike layer on ice surfaces [5]. Ellipsometry experiments disclosed no changes in the optical constants on the basal surface, i.e., no waterlike surface layer, below $-1\,^{\circ}\mathrm{C}$ [6–8], on the prism surface, a change in the ellipsometry signal which occurs roughly around $-4\,^{\circ}\mathrm{C}$ has been interpreted in terms of surface melting [6,7]. A rather controversial picture has been obtained from ion scattering experiments [9] which probe surface-related local order. Here the authors found a disordered surface layer already at $-54\,^{\circ}\mathrm{C}$ which grows to a thickness of 800 Å at $-1.8\,^{\circ}\mathrm{C}$.

Since the relevant order parameter of the solid-liquid transition is the set of Fourier components of the solid density-density correlation function, or in other words, the associated set of Bragg scattering intensities, the most direct and unambiguous experimental evidence of surface melting is provided by surface-sensitive Bragg scattering of x rays (Fig. 1): In this experimental setup a well-collimated, monochromatic x-ray beam hits the surface under a glancing angle α_i below the critical of total external reflection (α_c) and is specularly reflected, thereby an evanescent x-ray field is created at the surface which decays exponentially versus depth. The Bragg scattering signal from this exotic wave field which carries the information on the surface-related long-range order (LRO) is refracted out of the surface at a glancing exit angle α_f.

We show below that the phenomenon of surface melting of ice is partly accompanied by a thermal faceting. Glancing angle diffraction of x rays is an ideal tool to pick up and disentangle both surface phenomena in a rather straightforward way: The evanescent Bragg scattering signal reads (for nonzero momentum transfer parallel to the surface, $\mathbf{Q}_\parallel \neq 0$) [10]

$$I(\mathbf{Q}_\parallel, Q_z') \sim I_0 |T_i T_f|^2 [\delta(\mathbf{Q}_\parallel - \mathbf{G}_{hkl}) e^{-|\mathbf{Q}_\parallel|^2 u_\parallel^2}] \times \left[\frac{1}{|1 - e^{iQ_z' a_z}|^2} e^{-2L_d |\mathrm{Im} Q_z'|} \right], \quad (1)$$

with Q_z' the (refracted) perpendicular momentum transfer with respect to the surface and $|\mathrm{Im} Q_z'|^{-1} \equiv \Lambda$ the associated effective escape depth of the scattered evanescent x-ray wave ("scattering depth") ranging in ice between 50 Å for $\alpha_{i,f} < \alpha_c$ and several 1000 Å for $\alpha_{i,f} > \alpha_c$. The damping factor $\exp(-2L_d |\mathrm{Im} Q_z'|)$ originates from a quasiliquid surface layer of thickness L_d and gives rise to a characteristic intensity drop which is most pronounced for small settings of $\alpha_{i,f}$. The presence of facets with various orientations with respect to the average surface, on the other hand, is directly observable in the optical part of Eq. (1): T_i and T_f are the transmission functions of the illuminated facets which produce characteristic intensity enhancements, whenever $\alpha_{i,f} = \alpha_c$. When several facets with discrete orientations are present, the different facet horizons give rise to well-separated α_f Bragg profiles.

Ice I_h single crystals were grown from "Millipore" water by zone refinement and subsequently cut by a heated

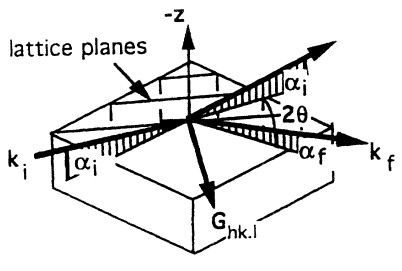

FIG. 1. Glancing angle scattering geometry ($\mathbf{k}_i$ and $\mathbf{k}_f$ are the wave vectors of the incident and scattered x-ray beam, and $\mathbf{G}_{hkl}$ a reciprocal lattice vector lying in the surface).

0031-9007/94/72(22)/3554(4)$06.00

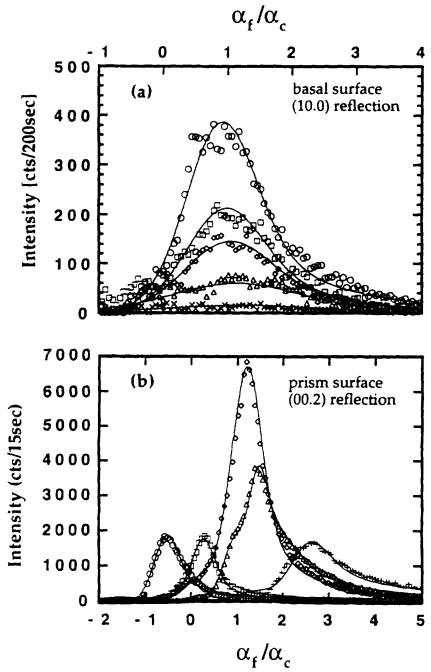

FIG. 2. Temperature of the α_f Bragg profiles together with theoretical fit within the DWBA: (a) (10.0) reflection observed at the basal surface for $T=-13.48\,^{\circ}\mathrm{C}$ (○), $-9.27\,^{\circ}\mathrm{C}$ (□), $-6.72\,^{\circ}\mathrm{C}$ (◇), $-4.46\,^{\circ}\mathrm{C}$ (△), and $-1.15\,^{\circ}\mathrm{C}$ (×). (b) (00.2) reflection observed at the prism surface for $T=-20.21\,^{\circ}\mathrm{C}$ (○), $-8.87\,^{\circ}\mathrm{C}$ (□), $-6.60\,^{\circ}\mathrm{C}$ (◇), $-3.81\,^{\circ}\mathrm{C}$ (△), and $-1.05\,^{\circ}\mathrm{C}$ (×).

wire. After a proper crystallographic orientation on a conventional x-ray diffractometer the crystals were mounted on an optical bench in a walk-in cold room, where the surface of interest was prepared by a mirrorlike, slightly heated glass plate which was softly pressed against the ice crystal. By slowly recooling the assembly the macroscopic melt between the crystal and the glass plate recrystallized perfectly. Before the actual x-ray experiment the glass plate was carefully taped off at $-6\,^{\circ}\mathrm{C}$, then the ice crystal with its optically flat surface was transferred in a thermally isolated x-ray chamber. The subsequent x-ray analysis revealed a mirrorlike single crystal surface with a mean surface roughness of $\langle\sigma\rangle=10$ Å and a waviness of $\Delta=1.1$ mrad as imposed by the glass surface. All glancing angle Bragg reflections exhibited in-plane mosaicities less than 0.02° and a perfect Q_z profile at low temperatures consistent with $L_d=0$. The key component of the x-ray chamber is a small, thermally isolated capsule which contains the sample and a vapor source 10 mm above the crystal surface, both thermoelectrically cooled. Within this capsule we control the sample temperature within $\pm 0.015°$ the vapor pressure, and the temperature of the gas phase. By this the sublimation rate of the sample surface (typically 3.5 μm/h) could be accurately adjusted, assuring that the ice surface was kept mirrorlike and clean throughout the entire experiment (for further details see [11]).

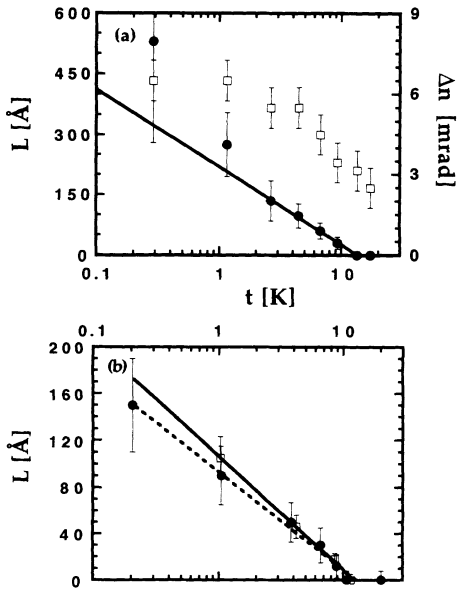

FIG. 3. (a) Thickness of the quasiliquid surface layer (●) and peak broadening (□) versus $\ln(T_m-T)$ as measured at the basal surface. (b) Thickness of the quasiliquid surface layer versus $\ln(T_m-T)$ as measured at the (10.0) (●) and (11.0) surface (□). The straight lines are the best least-squares fits to the data implying $L\sim\ln|1/t|$ consistent with wetting theory.

The x-ray scattering experiments have been performed during several experimental runs at the Hamburg Synchrotron radiation laboratory (HASYLAB at DESY, Hamburg) using monochromatic x rays ($\lambda=1.5$ and 1.735 Å) at the surface diffractometers of the W1 and the newly installed BW6 station. We have investigated the [00.1] ("basal"), [10.0] ("prism"), and [11.0] surfaces [12] for various incidence angles in a temperature range between $-20\,^{\circ}\mathrm{C}$ and the ice melting point. By way of example the α_f profiles of the (10.0) reflection at the basal surface and the (00.2) reflection at the prism surface are shown in Fig. 2 for various temperatures below $0\,^{\circ}\mathrm{C}$ and for $\alpha_i=0.8\alpha_c$ and $0.7\alpha_c$ together with theoretical models (full lines). After noting that such α_f profiles can simply be converted in Q_z profiles for a given α_i we turn now to the basal surface [Fig. 2(a)]: Upon approaching the melting point we find that the intensity decays by a factor of $\simeq 20$ between $-13.48°$ and $-1.15\,^{\circ}\mathrm{C}$ which is way beyond the expected thermal Debye-Waller factor giving rise only to a mild overall intensity decrease by 5% within this temperature interval. Thus, this x-ray observation is a clear surface disordering effect upon the in-plane translational order of ice. A least-squares fit analysis confirms indeed that the recorded intensity drop is best understood by introducing the damping factor $\exp(-2L_d|\mathrm{Im}Q_z'|)$ associated with a quasiliquid surface layer. The resulting thickness L_d is shown in Fig. 3(a) (full symbols) versus $t\equiv T_m-T$ (T_m is the melting temperature) on a semilogarithmic scale implying that the basal surface remains ordered up to the so-called onset

temperature of surface melting, $T_s = -13.5 \pm 2.5\,^{\circ}\mathrm{C}$, where a disordered surface layer appears which grows in thickness up to 500 Å at $-0.3\,^{\circ}\mathrm{C}$. For the interpretation of this large surface effect another direct x-ray observation is most important, the temperature-dependent change in the width of the α_f profiles [open symbols in Fig. 2(a)] which is, as the intensity change discussed before, completely reversible with temperature. At first sight two surface phenomena can be envisaged to cause this change in the scattering profiles: the appearance of water droplets with a shallow contact angle on top of the surface melt or strong fluctuations of the solid-quasiliquid interface. The first phenomenon, caused by blocked surface melting due to long-ranged van der Waals (vdW) interactions, has indeed been suggested to occur at ice surfaces [13], however, since we kept our samples slightly (but safely) undersaturated, the formation of such nonequilibrium droplets can be excluded in our case. The observation that the thickness of the wetting layer grows according to

$$L_d \sim l_d \ln[1/t] \tag{2}$$

[straight line in Fig. 3(a)] also tells us that the regime $L_d < 200$ Å is not dominated by long-ranged vdW, but by exponentially decaying interactions [14]. The continuous change in the peak width [Fig. 2(a)] speaks in favor of a gradual onset of interfacial fluctuations upon increasing the thickness of the liquid film. Following mean field theory [14] Eq. (2) is essentially preserved in the case of Gaussian fluctuations, however, the growth amplitude l_d is predicted to be no longer given by the correlation length ξ_d of the liquid phase (see below), but to scale with $(kT/\gamma_{sl})^{1/2}$. Simultaneously, the width of the solid-liquid interface should grow as $[\ln|1/t|/\gamma_{sl}]^{1/2}$. The interfacial energy γ_{sl} between ice and the quasiliquid is not known experimentally, but can be estimated by counting the effective number of broken bonds [15]. With the well-known latent heat of melting we find $\gamma_{sl} \simeq 15$ mJ/m^2 compared to $\gamma_{sv} = 120$ and 128 mJ/m^2 associated with the solid-vapor interface of the basal and prism surfaces, respectively. Consequently, the solid-liquid interface is expected to be rather diffuse, and the amplitude of the thickness growth to be strongly enhanced. The latter can be deduced from the slope of the straight line in Fig. 3(a) giving a large value of 84^{+43}_{-14} Å (for $L_d > 2000$ Å deviations from the $\ln|1/t|$ behavior are detected).

A somewhat different surface melting scenario is found at the nonbasal surfaces, where an additional thermal faceting takes place. Figure 2(b) depicts some typical α_f spectra as observed at the prism surface for some selected temperatures together with theoretical fits (full lines). The various separated α_f profiles which occur upon heating are associated with different facets emerging at the prism surface which exhibits a miscut angle of $\Delta\phi = 6.7$ mrad between the [10.0] surface normal and the [00.1] in-plane direction. A detailed analysis of the scattering distribution implies that the prism surface decomposes almost completely into ideal [10.0] facets already at $-20\,^{\circ}\mathrm{C}$. Upon heating they are replaced by a facet distribution around the average (vicinally cut) surface. The different facet horizons can readily be deduced from the individual α_f profiles in Fig. 2(b) (for the analysis of the facet orientation see Ref. [11]). The details of thermal faceting will be described in a forthcoming paper [16]; here we focus on the surface melting aspect. The intensity and shape analysis of the individual α_f profiles clearly indicate the appearance of disordered surface layers on top of the ice facets. The thickness L_d of the surface disorder as deduced from the semikinematic analysis [full lines in Fig. 2(b)] is shown in Fig. 3(b) versus t on a semilogarithmic plot: The prism and the [11.0] surface remain ordered up to $T_s = 12.5\,^{\circ}\mathrm{C}$; upon further heating the thickness of the quasiliquid gradually increases. The growth law of the disordered layers obeys again in a good approximation a $\ln|1/t|$ law [straight lines in Fig. 3(b)] with growth amplitudes $l_d = 42 \pm 9$ and 36 ± 8 Å for the [11.0] and [10.0] surfaces, respectively, which are in both cases larger than the bulk correlation length in water [17], $\xi_d \simeq 8$ Å. This indicates again the action of soft interfacial fluctuations and/or the presence of an enlarged correlation length within the surface melt. The latter implies that the supercooled melt which emerges in a surface layer of mesoscopic thickness is not a simple liquid, in particular, it is more correlated than bulk water [18], a fact which would explain why ellipsometry measurements never picked up a surface melting signal in this temperature regime. Incidentally it should be noted here that undersaturation also leads to an enhancement of l_d [19]; the effect, however, even in the case of ice, is negligibly small.

Ice as purely hydrogen-bonded matter has been considered for many decades as a model system to study the nature of the hydrogen bond which plays a vital role in biochemistry. The famous intrinsic bulk disorder of the hydrogen bonds in ice is assumed to play a fundamental role for many properties of ice, in particular for its stability; thus, one may speculate as to whether the observed disappearance of translational order at the surface of ice may be mediated by a surface-induced breakdown of the LRO between the hydrogen-bonding network. Since x-ray scattering from H_2O is dominated by the oxygen, H-H correlations are only accessible for x rays at those singular momentum transfers, where the scattering amplitudes of the oxygen atoms just cancel each other. This situation occurs at ($hk.4$) Bragg points which are oxygen forbidden. In this study we investigate the (00.4) point: The bulk reflection is shown in Fig. 4(a) exhibiting an angular width as small as 0.01° (resolution limited). At the (10.0) surface the same reflection has been measured between $-20\,^{\circ}\mathrm{C}$ and the melting point at glancing angles. Figure 4(b) shows typical in-plane angular scans through the (00.4) reciprocal lattice vector at various temperatures. Surprisingly, we found no δ-function contribution at all, but a Lorentzian-type scattering law with a typical angular width of 1.5° (FWHM) in striking contrast to

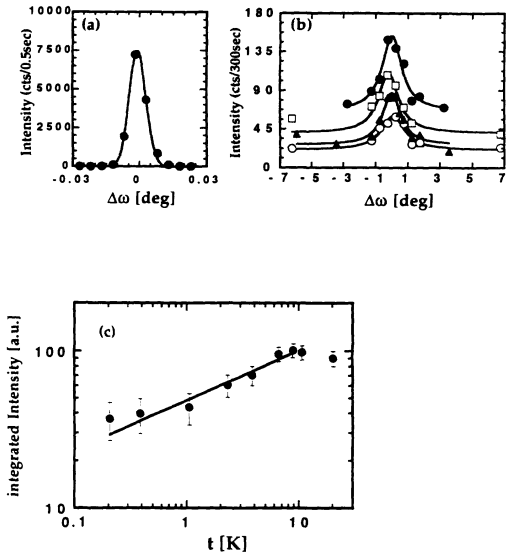

FIG. 4. X-ray measurements of the oxygen-forbidden (00.4) Bragg intensity: (a) Angular scan as measured in the bulk (full curve is a Gaussian fit accounting for instrumental resolution). (b) Angular scan under glancing angles as measured at the prism surface for $T=-10.68\,^{\circ}\mathrm{C}$ (●), $-3.81\,^{\circ}\mathrm{C}$ (□), $-2.31\,^{\circ}\mathrm{C}$ (▲), and $-0.39\,^{\circ}\mathrm{C}$ (○) (the full lines are Lorentzian fits). (c) Temperature dependence of the integrated Lorentzian intensity; the full line is a power law fit $t^{2\beta}$ yielding $\beta=0.16$.

the aforementioned resolution-limited widths of the glancing angle structural reflections. This observation implies that the surface-dominated H-H correlations exhibit a strong rotational disorder. As temperature increases, the integrated intensity underneath the Lorentzian line starts to decay strongly at $T\simeq -10\,^{\circ}\mathrm{C}$ [Fig. 4(c)], thereby following in a good approximation $I\sim|t|^{2\beta}$ (full line) with $\beta=0.16$. As this power law behavior is only consistent with

$$I\sim\exp(-2L_d|\mathrm{Im}Q_z'|)$$

which holds quite generally in the presence of surface disorder [Eq. (1)], when $L_d=(\beta/|\mathrm{Im}Q_z'|)\ln|1/t|$, we find again a $\ln|1/t|$ growth mode for the surface-induced disruption of the hydrogen-bonding network with a growth amplitude $l_d=\beta/|\mathrm{Im}Q_z'|$ being $l_d=45\pm15$ Å in our case. The so-deduced growth law agrees in essence with the one observed for the disappearance of translational order (as discussed above); thus, we conclude that the surface-induced disorder of the hydrogen bonds appears prior to the actual surface melting. Furthermore, detailed experimental studies which are currently being planned should shed more light on this fascinating new surface phenomenon.

We thank H. Peisl for his support and the HASYLAB staff for technical assistance during our experiments. M. Roesner and H. Rhan assisted during the experiments at HASYLAB. This work was supported by the Bundesminister für Forschung und Technologie under Grants No. 03PE1LMU and No. 03PE1LMU2.

*Present address: Institut für Materialwissenschaften, Bergische Unviersitaet Wuppertal, 42285 Wuppertal, Germany.

[1] M. Faraday, Philos. Mag. **17**, 162 (1859).
[2] G. J. Turner and C. D. Stow, Philos. Mag. **49**, L25 (1983).
[3] T. Kuroda, J. Phys. C **1**, Suppl. 3, 487 (1987); J. G. Dash, in *Phase Transitions in Surface Films 2*, edited by H. Traub, G. Torzo, H. J. Lauter, and S. C. Fain, NATO ASI Ser. B, Vol. 267 (Plenum, New York, 1991).
[4] J. J. De Koning, G. De Groot, and G. J. Van Ingen Schenau, J. Biochem. **25**, 565 (1992).
[5] H. H. G. Jellinek, J. Colloid Interface Sci. **25**, 245 (1967).
[6] D. Beaglehole and D. Nason, Surf. Sci. **96**, 357 (1980).
[7] Y. Furukawa, M. Yamamoto, and T. Kuroda, J. Cryst. Growth **82**, 665 (1987).
[8] M. Elbaum, S. G. Lipson, J. G. Dash, J. Cryst. Growth **129**, 491 (1993).
[9] I. Golecki and C. Jaccard, J. Phys. C **11**, 4229 (1978).
[10] H. Dosch, *Critical Phenomena at Surfaces and Interfaces*, Springer Tracts in Modern Physics Vol. 126 (Springer, Berlin, 1992).
[11] A. Lied, H. Dosch, and J. H. Bilgram, Physica B (to be published).
[12] We use the traditional crystallographic (*hk.l*) notation in ice physics, where *l* points in the *c* direction (normal to the basal plane) and *h*,*k* are nonorthogonal vectors in the basal plane.
[13] M. Elbaum and M. Schick, Phys. Rev. Lett. **66**, 1713 (1991).
[14] R. Lipowsky, Ferroelectrics **73**, 69 (1987).
[15] T. Kuroda and R. Lacmann, J. Cryst. Growth **56**, 189 (1982).
[16] A. Lied, H. Dosch, and J. H. Bilgram (to be published).
[17] A. H. Narten and H. A. Levy, *The Physics and Physical Chemistry of Water*, edited by F. Franks (Plenum, New York, 1972), Vol. 1.
[18] For the possibility of an enhanced bulk correlation length upon supercooling see, e.g., P. H. Poole, F. Sciortino, U. Essmann, and H. E. Stanley, Nature (London) **360**, 324 (1992).
[19] H. Löwen and R. Lipowsky, Phys. Rev. B **43**, 3507 (1991).